

Spatial and Temporal Sensitivity of X- and Y-Cells in Dorsal Lateral Geniculate Nucleus of the Cat

STEPHEN LEHMKUHLE, KENNETH E. KRATZ, STUART C. MANGEL, AND S. MURRAY SHERMAN

Department of Physiology, University of Virginia School of Medicine, Charlottesville, Virginia 22908

SUMMARY AND CONCLUSIONS

1. We measured spatial and temporal sensitivity of 81 X-cells and 46 Y-cells in the lateral geniculate nucleus of cats by determining contrast thresholds of single cells to counterphased, sine-wave gratings. The plots of contrast sensitivity (reciprocal of the contrast threshold) as a function of spatial or temporal frequency of the sine-wave grating represent the contrast sensitivity functions.

2. The spatial contrast sensitivity functions were measured at a temporal frequency (counterphase rate) of 2 cycles/s. The shape of the function for X-cells was an inverted U. Contrast sensitivity peaked around 0.5–1.0 cycles/deg, and decreased at lower and higher spatial frequencies. Contrast sensitivity of Y-cells was highest at low spatial frequencies, and systematically declined at higher spatial frequencies. By virtue of the relative shapes of these functions, Y-cells were more sensitive at low spatial frequencies than were X-cells. At high spatial frequencies, X-cells were slightly more sensitive. Spatial resolution, defined as the highest spatial frequency to which the cell responded at 0.6 contrast, declined monotonically with eccentricity of receptive-field location from the area centralis for both X- and Y-cells, and X-cells had a slightly higher average resolution than did Y-cells at most eccentricities.

3. Temporal contrast sensitivity functions were measured using the spatial frequency to which the cell exhibited the lowest contrast threshold. The shapes of the

temporal functions were similar for both X- and Y-cells. Both cell groups exhibited the highest sensitivity at low temporal frequencies and systematic decreases in sensitivity at higher temporal frequencies. The temporal resolution, which was the highest counterphase rate to which the cell responded at 0.6 contrast, was higher for Y-cells than for X-cells within the binocular segment (0–40° eccentricity). In the monocular segment, there was no obvious difference in temporal resolution between X- and Y-cells. For both X- and Y-cells, temporal resolution was fairly constant for all receptive-field eccentricities within the binocular segment.

4. Spatiotemporal interactions were investigated by measuring spatial contrast sensitivity functions at a number of temporal frequencies, in addition to 2 cycles/s. Contrast sensitivity was attenuated for all spatial frequencies at higher temporal frequencies; however, the shape of the spatial functions for both X- and Y-cells was preserved.

5. Grating position within a receptive field was found to be an important factor in the measurement of contrast thresholds for all spatial frequencies for X-cells and for low spatial frequencies for Y-cells. However, at higher spatial frequencies, the thresholds of Y-cells were position independent. Within Y-cells, the nonlinear subunits (17, 18) exhibited higher spatial and lower temporal resolution than did the linear center/surround portion of the field.

6. Receptive-field center diameter, measured by hand plotting or estimated from

area-response functions, correlated weakly with spatial resolution. Area-response functions indicated a strong center-surround antagonism in X-cells and a weak center-surround interaction in Y-cells. This result was related to the different shapes of the spatial contrast sensitivity functions.

7. It is suggested that Y-cells mediate basic spatial pattern vision mainly because of their superior sensitivity to lower spatial frequencies and lack of specificity for stimulus position. It is suggested that X-cells provide fine spatial detail and position information.

INTRODUCTION

During the past decade, a great deal of attention has been focused on the different functional neuron populations in the mammalian retinogeniculocortical pathways (34, 35). Most studies have concentrated in cats upon two of these populations, commonly termed X- and Y-cells.¹ These cells, which occur both in retina and the lateral geniculate nucleus, differ among a number of physiological characteristics (7, 10, 17, 18, 20, 36), but the significance for visual function of these different properties is far from clear. One reason for this is the difficulty in relating receptive-field data, on the one hand, to behavioral or psychophysical data, on the other hand, since these approaches tend to have little in common.

As in other recent approaches (2, 6, 10, 30–33, 36), we sought to bridge this gap somewhat by obtaining receptive-field data from cat geniculate X- and Y-cells with stimulation techniques that are common to many psychophysical approaches and thus provide clearer insights into the different functional roles of X- and Y-cells. That is, we measured spatial and temporal contrast sensitivity for individual neurons to a stimulus consisting of counterphased, sine-wave gratings. Sensitivity was measured for

a wide range of spatial and temporal parameters. These same general stimulus configurations have been used in cats (3, 4) and humans (Ref. 27; and many others) to obtain psychophysically measured contrast sensitivity. Our results, which confirm and extend the observations of previous studies (10, 17, 18, 23, 30) indicate clear but complex differences between X- and Y-cells in terms of their sensitivity to spatial and temporal patterns.

MATERIALS AND METHODS

Animal preparation and recording methods

We studied response properties of single geniculate neurons in normal adult cats. Our methods have been described in detail elsewhere (20, 25, 28) and will be briefly summarized here. The cats were anesthetized with halothane for initial surgery and maintained on N₂O/O₂ (70/30) during the recording session. They were paralyzed with a continuous infusion of gallamine triethiodide and tubocurarine, artificially ventilated, and had end-tidal CO₂ maintained at 4%. After topical application of atropine and Neo-Synephrine onto the eyes, the corneas were covered with contact lenses. Retinoscopy was used to ensure conjugacy of each retina with the visual stimuli (usually on a cathode-ray tube (CRT) face placed 57 cm in front of the eyes), and 3-mm-diameter artificial pupils were employed to optimize the optics. Retinoscopy was employed along peripheral axes to ensure that retinal regions under study, regardless of eccentricity, were conjugate with the stimuli.

We used varnish-insulated tungsten microelectrodes or NaCl-filled micropipettes (usually 10–40 MΩ at 500 Hz) to record extracellular potentials from single geniculate neurons in laminae A and A1. Bipolar stimulating electrodes were inserted to straddle the optic chiasm. Square-wave pulses (typically ≤5 mA for ≤50 μs) were applied across these electrodes to activate geniculate neurons orthodromically. Once a geniculate cell was isolated for study, its receptive-field position, polarity (i.e., on- or off-center), and diameter were determined. The neuron was then identified as an X- or Y-cell with a standard battery of tests, which included: response latency to optic chiasm stimulation, the linearity of spatial summation, and responsiveness to fast-moving (>200°/s) targets (10, 17, 18, 20, 26). No W-cells were identified, presumably because they are found nearly exclusively in the C-laminae (8, 40), and the cells of the present study were located in the A-laminae. For most of these

¹ Three neuron classes have been identified in the cat's retinogeniculocortical pathways, including W-, X-, and Y-cells. Least is known about the properties of geniculate W-cells, but they seem to be limited to the C-laminae (8, 40). Unlike X- and Y-cells, W-cells tend to respond in a very sluggish fashion, to have poor center/surround antagonism, and to have very slowly conducting axons.

neurons, the receptive-field diameter was measured with hand-plotting techniques (20), but for some, area-response functions (cf. Ref. 21) were determined to obtain a more quantitative measure of this diameter. For these functions, CRT-generated circular targets of 33 cd/m² against a background of 1.0 cd/m² were flashed on and off at a rate of 2 cycles/s. A computer was used to measure neuronal response (in spikes/s) as a function of target size.

Spatial and temporal contrast sensitivity functions

Vertically oriented sine-wave gratings were generated on a CRT to determine neuronal sensitivity to spatial and temporal modulations of contrast. We were able to control independently the stimulus contrast ($(L_{\max} - L_{\min}) / (L_{\max} + L_{\min})$), where L_{\max} and L_{\min} refer, respectively, to maximum and minimum luminance), spatial frequency (cycles/deg), temporal frequency (cycles/s), and the spatial phase angle relative to the CRT face or receptive-field location. Temporal modulation usually was achieved by square-wave counterphasing of the grating; in some cases, sine-wave counterphasing was also used to generate temporal modulation. The CRT display was 4° × 6° (at the 57-cm viewing distance) and had a space average luminance ($\frac{1}{2}(L_{\max} + L_{\min})$) of 33 cd/m². Contrast values could be continuously varied between 0 and 0.6. For a given spatial and temporal frequency, contrast was adjusted until a threshold neuronal response was obtained, and in this manner contrast sensitivity (the inverse of the contrast threshold) was plotted for a range of spatial and temporal variables. For some cells, computer-generated peristimulus histograms were used to determine the neuronal response to the grating stimuli, but in most cases, the thresholds were determined by listening to the audio monitor output of the cell's response (see RESULTS).

RESULTS

Response properties were determined for 81 X-cells and 46 Y-cells from laminae A and A1 in 15 normal adult cats. Their receptive fields were all within ±25° of the horizontal zero parallel, and ranged from the area centralis to 89° eccentric. For many of these cells (44 X-cells and 31 Y-cells), complete spatial and temporal contrast sensitivity functions were determined with counterphased, sine-wave gratings. No differences between cells located in laminae A and A1 were found for any of the response properties measured (see, however, Ref. 19), so

data are pooled across these laminae. Furthermore, no differences in spatial or temporal contrast sensitivity were found between on- and off-center cells, so again, these data are pooled.

Measurements of spatial and temporal contrast sensitivity

The gratings were generated on a CRT face appropriately positioned so that the receptive field was placed in its center. A low spatial frequency grating (≤ 0.25 cycles/deg), counterphased at 2 cycles/s, had its spatial phase shifted until the neuron either ceased responding (i.e., a "null" position for an X-cell) or produced a symmetrical "doubling" or "second harmonic" response at twice the stimulus temporal frequency (for a Y-cell). Our results conform closely to the model proposed by Hochstein and Shapley (17, 18). That is, with our contrast and luminance levels, X-cells responded fairly linearly and only at the fundamental frequency of the stimulus. This linear, fundamental response could be canceled by appropriate placement of the grating (i.e., the null position). Y-cell fields seem to be comprised both of a linear center/surround organization, which responded only at the fundamental stimulus temporal frequency, and also of superimposed, nonlinear spatial subunits, which responded at twice the stimulus temporal frequency. These latter subunits are responsible for the second harmonic response. Appropriate grating placement could cancel the linear, fundamental response, leaving only the second harmonic response (see Refs. 17, 18 for details).

Once the spatial phase angle that failed to evoke the fundamental response was determined, the grating was shifted in spatial phase by 90° for determinations of contrast sensitivity. This maximized the neuronal response. The spatial phase angle of the grating was repeatedly checked to control for small eye movements. The fundamental response of Y-cells ceased at higher spatial frequencies. This occurs presumably because the linear components of Y-cells are less sensitive to high spatial frequencies than are the nonlinear subunits (see below and Refs. 17, 18). Since this left only the second harmonic response, which was inde-

pendent of stimulus spatial phase, adjustments of spatial phase angle became unnecessary for Y-cells at higher spatial frequencies.

Spatial contrast sensitivity functions were first plotted at a counterphase rate of 2 cycles/s because all cells in our sample responded vigorously at that temporal frequency. We measured each neuron's spatial

resolution, defined as the highest spatial frequency to which the cell responded, by increasing spatial frequency at our highest contrast level (0.6) until the neuron ceased responding in a discernibly modulated fashion. The spatial frequency at that point was identified as the neuron's spatial resolution (Figs. 1A, 2A). Contrast sensitivity

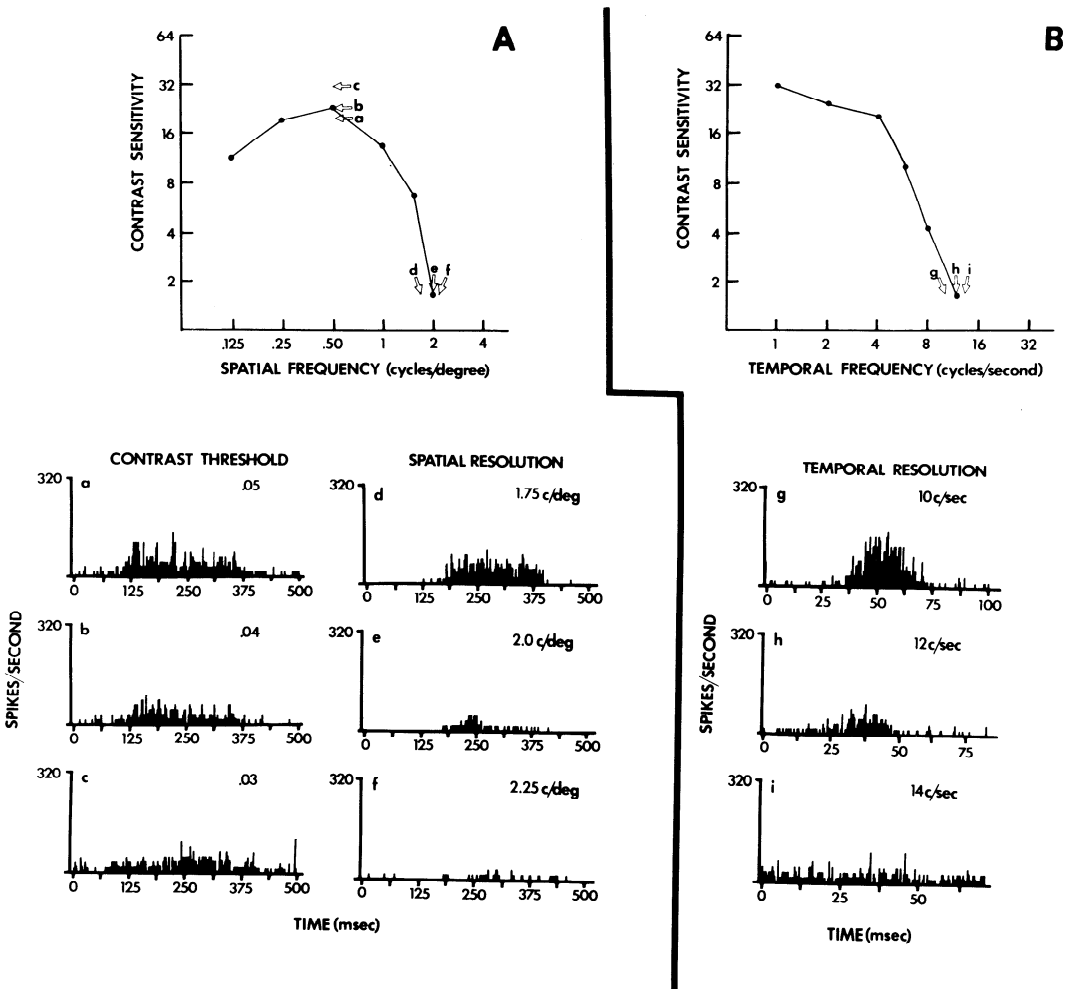


FIG. 1. Spatial (A) and temporal (B) contrast sensitivity functions for an X-cell. These curves plot contrast sensitivity, which is the reciprocal of the contrast threshold, as a function of either spatial or temporal frequency. Functions were derived from listening to the audio monitor output of the neuronal discharge (see text). Peri-stimulus histograms, which plot firing rate as a function of the stimulus cycle (one counterphase cycle is represented), are shown in the lower part of this figure. They were collected at several contrasts, spatial frequencies, and temporal frequencies, which bracket some of the threshold measurements derived by the listening procedure. Histograms a–f were collected at a temporal stimulus of 2 cycles/s. Histograms a, b, and c were collected using contrasts of 0.05, 0.04, and 0.03, respectively, at a spatial frequency of 0.5 cycle/deg. The contrast threshold for the cell at this spatial frequency was determined by the listening procedure to be 0.04. Histograms d, e, and f were collected at spatial frequencies of 1.75, 2.0, and 2.25 cycles/deg, all with a contrast of 0.6. The spatial resolution of the cell was determined by the listening procedure to be 2.0 cycles/deg. Histograms g, h, and i were collected at temporal frequencies 10, 12, and 14 cycles/s, respectively, all with a spatial frequency of 0.5 cycle/deg and at a contrast of 0.6. The temporal resolution of the cell was determined by the listening procedure to be 12 cycles/s.

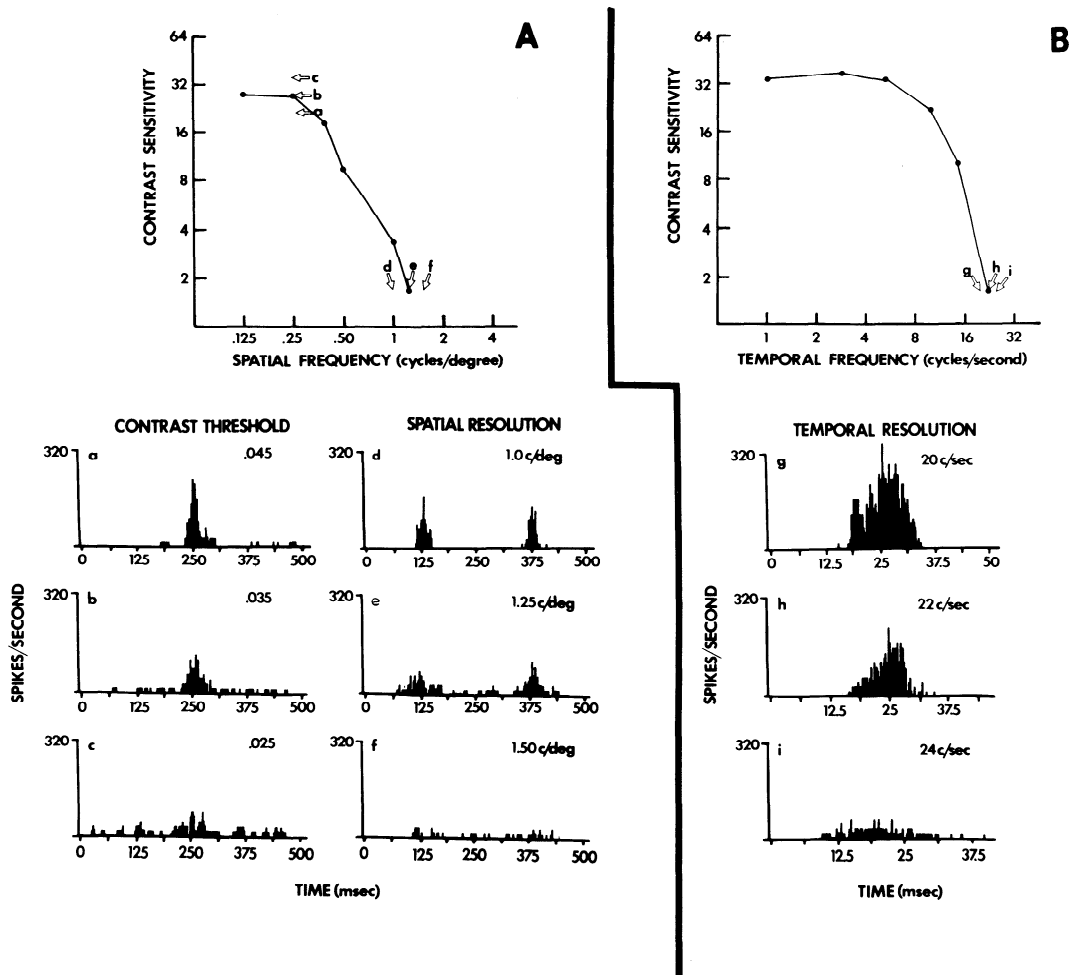


FIG. 2. Spatial (A) and temporal (B) contrast sensitivity functions for a Y-cell. See Fig. 1 for a more complete description. Peristimulus histograms a-f were collected at a temporal stimulus rate of 2 cycles/s. Histograms a, b, and c were collected, respectively, at contrasts of 0.045, 0.035, and 0.025, using a spatial frequency of 0.25 cycle/deg. The contrast threshold for the cell at this spatial frequency was 0.035, as determined by a listening procedure. Histograms d, e, and f were collected at spatial frequencies of 1.0, 1.25, and 1.50 cycles/deg, respectively, all at a contrast of 0.6. The spatial resolution of the cell as determined by the listening procedure was 1.25 cycles/deg. Histograms g, h, and i were collected at temporal frequencies of 20, 22, and 24 cycles/s, all at a spatial frequency of 0.25 cycle/deg and a contrast of 0.6. The temporal resolution determined from the audio monitor was 22 cycles/s. Note that histograms a, b, g, and h show a response dominated by one peak (i.e., a fundamental response); histograms d and e show responses at twice the stimulus frequency (i.e., second harmonic responses).

was then determined at 2 cycles/s for a range of lower spatial frequencies by noting the contrast threshold for each of these frequencies.

After the spatial contrast sensitivity function was plotted, the spatial frequency to which the cell was most sensitive (i.e., had the lowest contrast threshold) was fixed while temporal frequency was varied.

Temporal contrast-sensitivity functions were thus obtained in a manner analogous to that just described for spatial functions. Temporal resolution, defined as the highest counterphase rate to which the cell could respond, was determined at 0.6 contrast. Contrast thresholds were then determined at a range of lower temporal frequencies. For some cells, possible spatial/temporal inter-

actions were investigated by obtaining spatial contrast sensitivity functions for a range of temporal frequencies.

Because of its convenience and reliability, we chose to adopt a qualitative procedure to determine neuronal contrast thresholds. That is, we based threshold determinations on the audio monitor output of the cell's response. We found that only slight adjustments of contrast, temporal frequency, or spatial frequency near threshold were sufficient to alter the cell's responsiveness between unambiguous stimulus-evoked discharges and no evoked activity. To obtain these contrast thresholds, we used a staircase procedure, whereby contrast levels were varied above and below threshold in smaller quantities until a narrow threshold range was determined. In this fashion, contrast sensitivity functions were reproducible both for a given observer and between observers.

We verified these determinations for several X- and Y-cells with computer assistance. Histograms, which related neuronal firing rate to the stimulus cycle, were collected at several points near threshold, and no discernible differences were seen between threshold determinations based on the audio monitor output and those based on such histograms. Typical examples are shown for an X-cell (Fig. 1) and a Y-cell (Fig. 2). For these histograms, we usually averaged responses for only 25 stimulus cycles. Undoubtedly, had we averaged for more sweeps, weaker responses would be detectable, and our absolute estimates of contrast threshold would be reduced. For this reason, absolute determinations of contrast threshold may be misleading since they depend on somewhat arbitrary definitions of the threshold response. This report focuses on the use of the same threshold criterion to elucidate relative differences in contrast threshold as a function of spatial frequency, temporal frequency, and/or neuron type (X- or Y-cell).

It is emphasized that, at higher spatial frequencies, Y-cell responses were essentially independent of spatial phase. Indeed, our determinations of spatial resolution and contrast sensitivity functions at higher spatial frequencies for these cells were in-

variant with spatial phase. In contradistinction, for X-cells and at lower spatial frequencies for Y-cells, spatial phase proved to be an important consideration and had to be carefully adjusted as described above.

Spatial contrast sensitivity

Figure 3 illustrates examples of contrast sensitivity functions for six X-cells. A striking feature of every X-cell in the binocular segment (i.e., with receptive fields within roughly 40° of the vertical meridian; cf. Refs. 20, 39) is the clear attenuation in sensitivity to low, as well as to high, spatial frequencies. This results in the characteristic inverted U-shaped spatial functions for X-cells. However, for three of the nine X-cells with receptive fields located in the monocular segment (i.e., more than 40° from the vertical meridian), no low spatial-frequency attenuation was detected). This could be an artifact of our stimulus conditions, which made it difficult to produce gratings at frequencies less than 0.125 cycles/deg. Since the entire spatial contrast sensitivity functions generally shift down in spatial frequency with increasing receptive-field eccentricity (see also below), the possibility exists that for spatial frequencies lower than 0.125 cycle/deg, these three X-cells would have exhibited reduced contrast sensitivity.

Figure 4 shows analogous examples of contrast sensitivity functions for six Y-cells. Unlike X-cells, none of the Y-cells in our sample exhibited reduced contrast sensitivity to low spatial frequencies.

Figure 5A plots contrast sensitivities that have been averaged for 30 X-cells and 19 Y-cells with receptive fields within 10° of the area centralis. The most striking difference in spatial contrast sensitivity between X- and Y-cells occurs for low spatial frequencies. Y-cells exhibit much greater sensitivity at these frequencies than do X-cells. A less striking difference occurs at higher spatial frequencies, for which X-cells tend to exhibit greater contrast sensitivity and better spatial resolution than do Y-cells if their fields occur at reasonably matched eccentricities (see Figs. 6 and 7). Even so, some Y-cells exhibit more sensitivity at higher spatial frequencies and better spatial

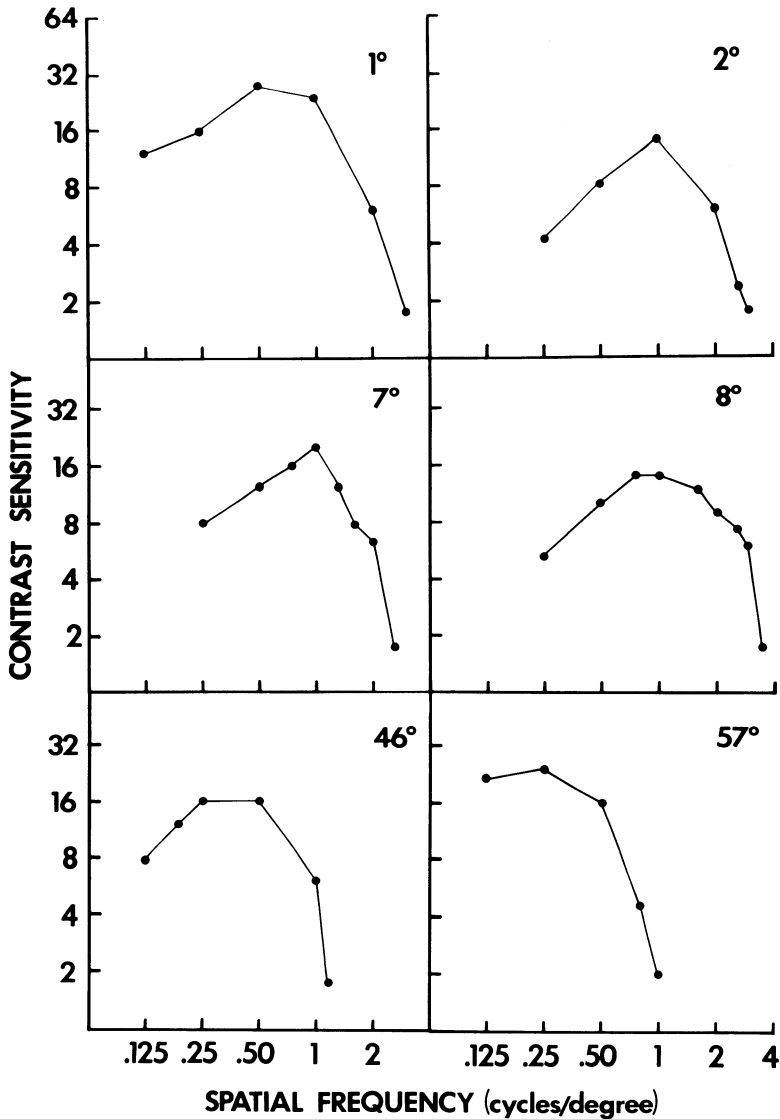


FIG. 3. Spatial contrast sensitivity functions for six X-cells. The number with each function denotes the eccentricity of the receptive field from area centralis.

resolution than do some X-cells. Therefore, at lower spatial frequencies, Y-cells are considerably more sensitive than are X-cells; and at higher spatial frequencies, X-cells tend to be slightly more sensitive than do Y-cells, although considerable variability is evident in this latter comparison.

The difference in sensitivity to higher spatial frequencies is further illustrated in Fig. 6. Here, the mean spatial resolution (± 1 standard error) as a function of receptive-field eccentricity is plotted separately for X- and Y-cells. Figure 7 shows for X- and

Y-cells the distribution of spatial resolution among single neurons both for the entire population and also for the separate eccentricity groups shown in Fig. 6. Three points emerge. First, considerable variability for this parameter exists among X- and Y-cells at any eccentricity. Second, for both cell types, resolution declines gradually with eccentricity ($P < 0.01$ on an F test), and the functions are roughly parallel for X- and Y-cells ($P > 0.10$ on an F test for interaction). Another consequence of this decline not illustrated is that the entire spatial con-

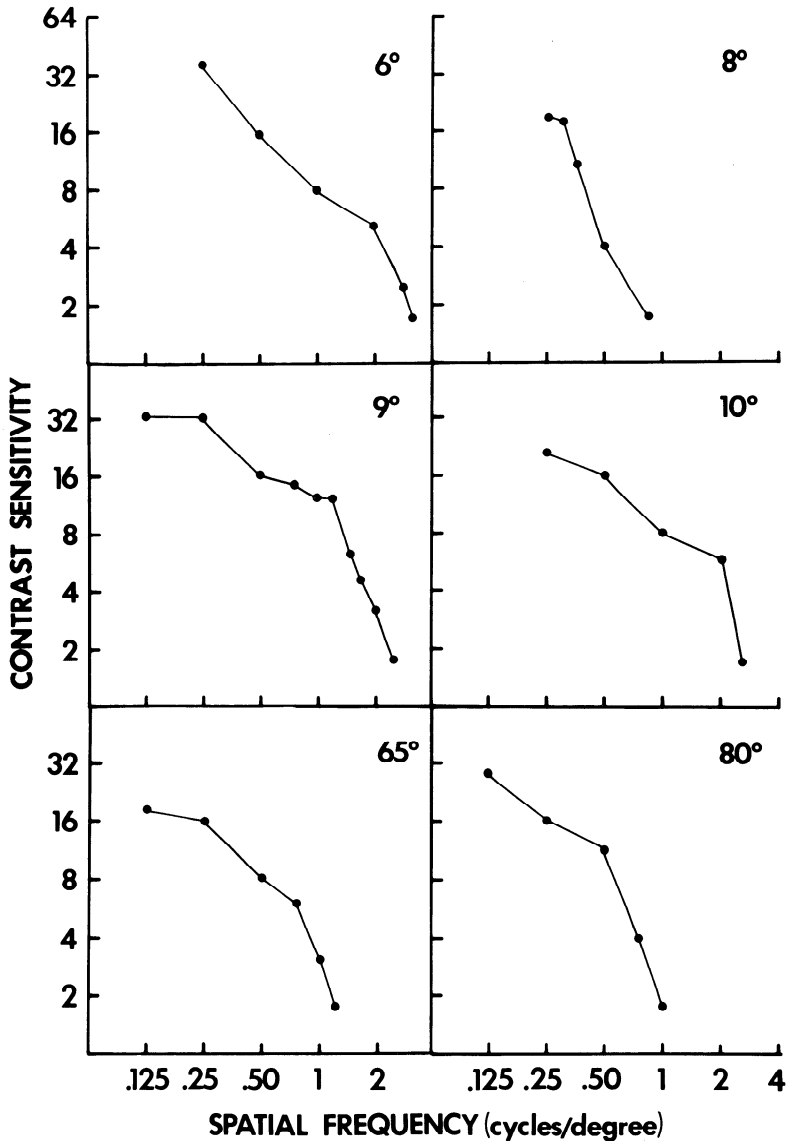


FIG. 4. Spatial contrast sensitivity functions for six Y-cells; conventions as in Fig. 3.

trast sensitivity functions shift downward on the spatial frequency domain with increasing eccentricity and, therefore, the most sensitive frequency for X-cells also declines with increasing eccentricity. Third, X-cells tend to have higher spatial resolution than do Y-cells ($P < 0.001$ on a Mann-Whitney U test for all cells), although at retinal eccentricity groups 0–5°, 10–15°, and 15–20°, the spatial resolution of X- and Y-cells do not statistically differ ($P > 0.10$ on a Mann-Whitney U test). However, Y-cells with more central fields typically have

better spatial resolution than do X-cells with more eccentric fields (see Fig. 6).

Temporal contrast sensitivity functions

Figure 8 illustrates temporal contrast sensitivity functions for six typical X-cells, and Fig. 9 shows analogous functions for six representative Y-cells. As mentioned above, these functions are generated at the most sensitive spatial frequency for each cell. For Y-cells, this most sensitive spatial frequency was always sufficiently low to involve responses at the fundamental spatial

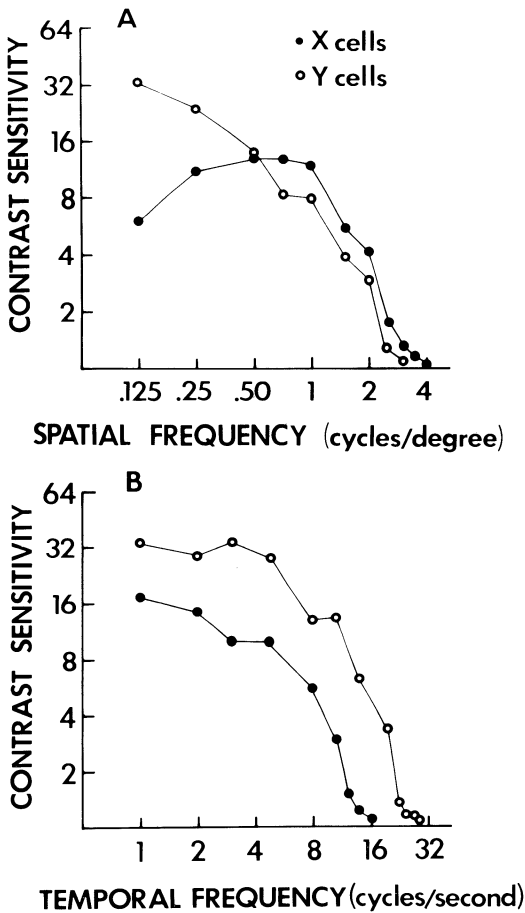


FIG. 5. Average spatial and temporal contrast sensitivity functions for X- and Y-cells. The spatial curves were determined by averaging contrast sensitivity values of 30 X-cells and of 19 Y-cells, and the temporal curves were determined by averaging contrast sensitivity values of 23 X- and of 14 Y-cells. All these cells had receptive fields within 10° of the area centralis. Filled circles denote average values for X-cells. Open circles denote average values for Y-cells. *A*: average spatial contrast sensitivity functions for X- and Y-cells. *B*: average temporal contrast sensitivity functions for X- and Y-cells.

frequency, so that responses were spatially phase dependent (cf. Refs. 17, 18). Therefore, our procedure for Y-cells measured temporal resolution of the fundamental response. In 10 Y-cells, we also measured temporal resolution of the second harmonic response by placing the grating in a position for which cells responded only in this fashion (i.e., the null grating position for the fundamental response). Interestingly, temporal resolution for the fundamental response was always greater than that for the

second harmonic response (on average, 23 versus 9.6 cycles/s; $P < 0.001$ on a Mann-Whitney U test). The Y-cell temporal resolutions indicated in Figs. 10 and 11 represent the fundamental responses.

As a consequence of the nature of the spatial contrast sensitivity functions (Figs. 3–5), it follows that higher spatial frequencies for these temporal functions were typically used for X-cells than for Y-cells. Y-cells tended to exhibit more sensitivity to higher temporal frequencies and a higher temporal resolution than did X-cells, but otherwise no obvious difference in these functions was evident. None of the geniculate X- or Y-cells studied showed a decreased sensitivity to lower temporal frequencies analogous to the attenuation in sensitivity at lower spatial frequencies for X-cells. Instead, both cell types exhibited characteristic increases without attenuation in contrast sensitivity at lower temporal frequencies and a systematic sensitivity attenuation at higher counterphase rates. Figure 5*B* illustrates the mean of the temporal contrast sensitivity determinations for 23 X-cells and 14 Y-cells.

The shape of these temporal contrast-sensitivity functions and, in particular, the

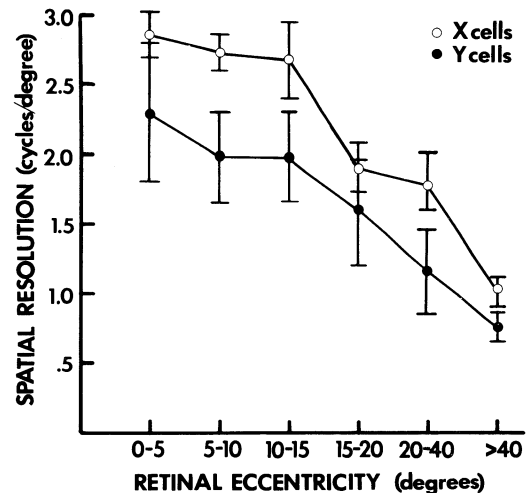


FIG. 6. Mean spatial resolution of X- and Y-cells plotted as a function of receptive-field eccentricity from area centralis. These were measured using a sine-wave grating of 0.6 contrast counterphased at 2 cycles/s (see text for details). Bars denote ± 1 standard error of the mean. Open circles indicate means for X-cells; filled circles, for Y-cells. The cell numbers represented by each point can be inferred from Fig. 7.

lack of low-frequency sensitivity attenuation, does not appear to be dependent on the square-wave counterphase function. For five X-cells and seven Y-cells, these functions were replotted with a sine-wave counterphase function, and no discernible change in these temporal contrast sensitivity functions resulted.

Figure 10 shows for X- and Y-cells the mean temporal resolution (± 1 standard error) at a contrast of 0.6 as a function of receptive-field eccentricity. Figure 11 shows the distribution of temporal resolution among the cells, both for the entire population and also separately for each of the eccentricity groups illustrated in Fig. 10. Throughout the binocular segment ($\leq 40^\circ$ eccentricity), these functions for X- and Y-cells are fairly flat, and Y-cells on average exhibit better temporal resolution than do X-cells ($P < 0.01$ on a Mann-Whitney U test for each eccentricity group, except $0-5^\circ$). Although some overlap between X- and Y-cells exists for this parameter, there is less than seen in terms of spatial resolution. Also, the flat nature of the curves in Fig. 10 within the binocular segment means that Y-cells tend to have better temporal resolution than X-cells, regardless of receptive-field location within this region.

A curious shift in temporal resolution occurs between the binocular and monocular segments. Relative to the binocular segment, monocular segment X-cells displayed higher temporal resolution, whereas the Y-cells showed lower temporal resolution. Consequently, no difference in mean temporal resolution was found between monocular segment X- and Y-cells ($P > 0.10$ on a Mann-Whitney U test). We cannot exclude the possibility that decreased temporal resolution was seen for monocular segment Y-cells because we were unable to stimulate at a spatial frequency lower than 0.125 cycle/deg, but this would not explain the increased resolution for X-cells here. Otherwise, we cannot account for or interpret this curious equivalence of X- and Y-cell temporal sensitivity in the monocular segment.

Spatiotemporal relationships

CORRELATIONS. From the above, it is evident that X-cells relative to Y-cells are more sensitive to higher spatial frequencies

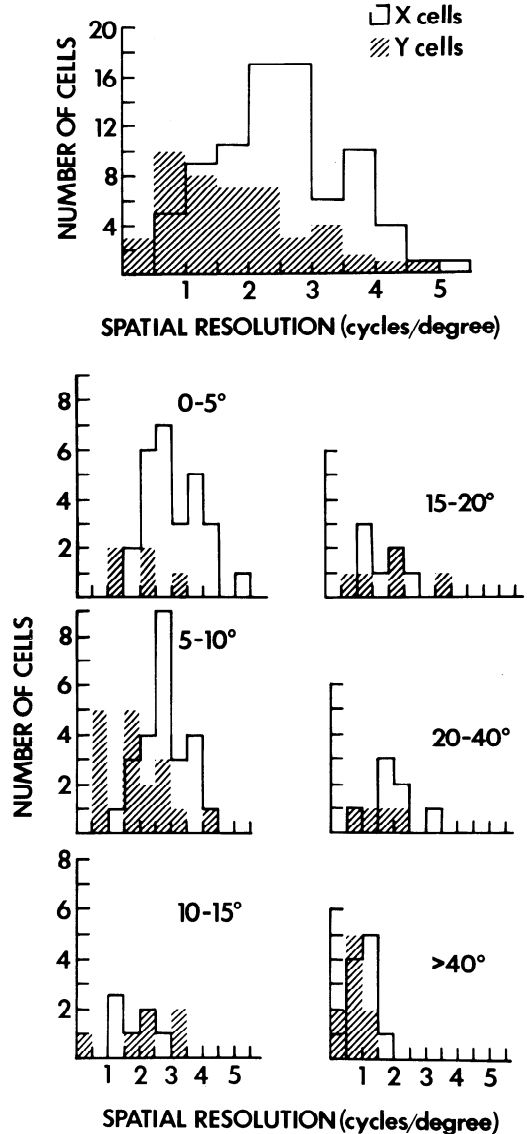


FIG. 7. Cell frequency distributions of spatial resolution for X- and Y-cells. The frequency distributions of spatial resolution for X- and Y-cells for all retinal eccentricities are shown in the upper part of the figure. The frequency distributions of X- and Y-cells for six different retinal eccentricity groups are separately shown in the lower part of figure. Open frequency histograms indicate distributions for X-cells; cross-hatched, for Y-cells.

and less sensitive to higher temporal frequencies. This could result partially from a reciprocal relationship between spatial and temporal sensitivity. Consequently, we searched for this within each cell group by plotting spatial versus temporal resolution for the individual neurons. For all X-cells, a

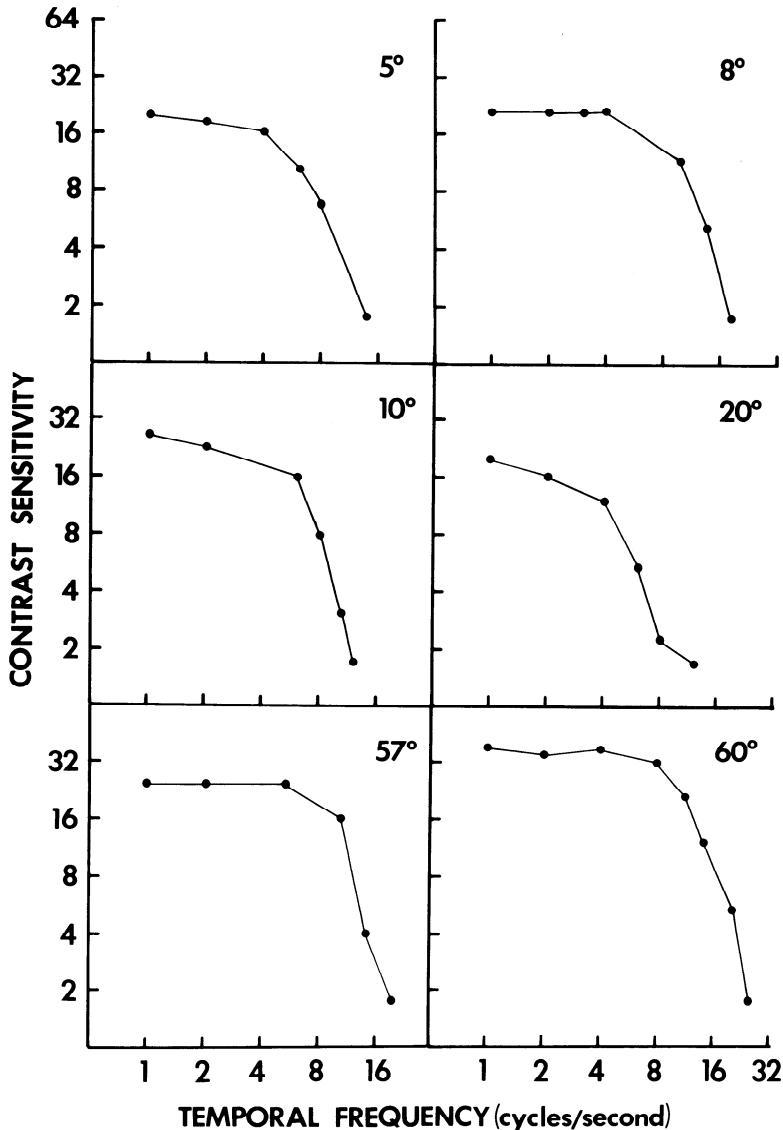


FIG. 8. Temporal contrast sensitivity functions for six X-cells. The number with each function denotes the eccentricity of the receptive field from area centralis.

weak negative correlation was found ($r = 0.38$; $P < 0.05$), whereas for all Y-cells, the weak correlation was positive ($r = +0.38$; $P < 0.05$). These correlations, however, are strongly influenced by data from the monocular segment and for reasons given above, we are somewhat skeptical of the relatively low temporal resolution for Y-cells. It seems appropriate to limit this analysis to data from the binocular segment. When this is done, no significant correlations are seen ($P > 0.10$ for each correlation). We were thus unable to obtain reasonable evidence

for a reciprocal relationship between spatial and temporal resolution within the X- or Y-cell populations.

INTERACTIONS. Spatial and temporal relationships for six X-cells and five Y-cells were measured in another fashion. For these cells, spatial contrast sensitivity functions were plotted for a range of temporal frequencies, in addition to 2 cycles/s. These data are illustrated for four X-cells in Fig. 12 and four Y-cells in Fig. 13. As indicated by the figures, no marked spatiotemporal

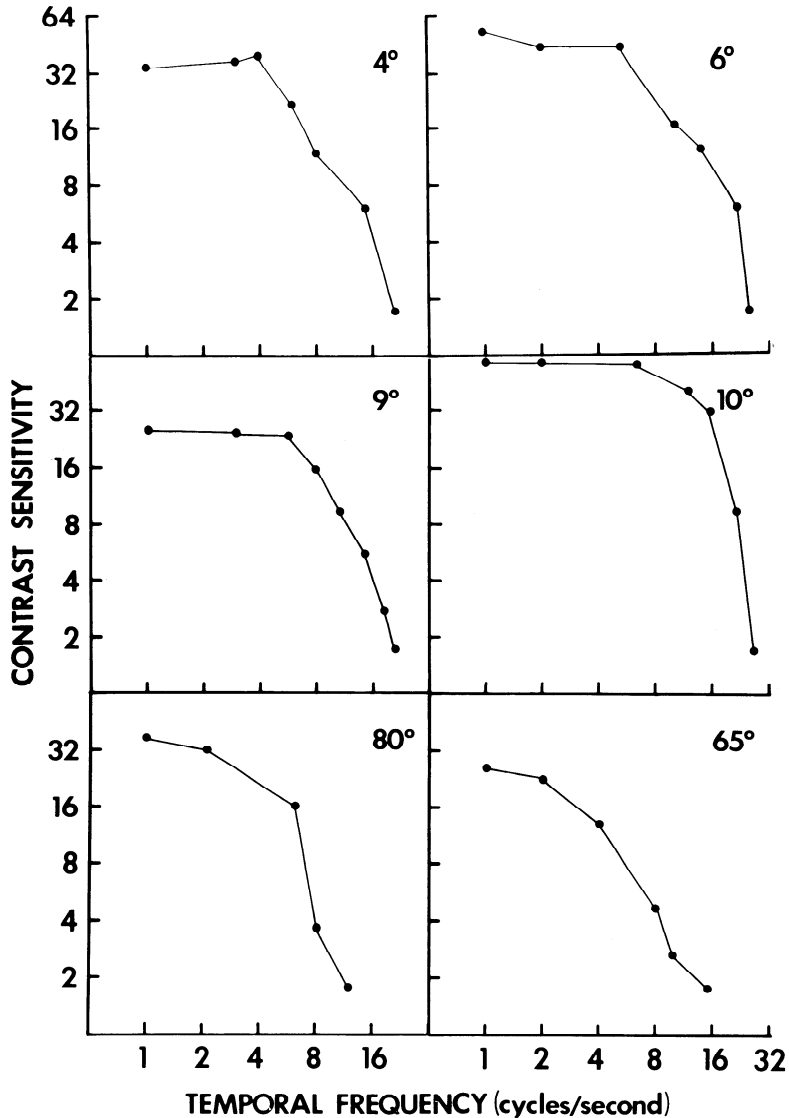


FIG. 9. Temporal contrast sensitivity functions for six Y-cells; conventions as in Fig. 8.

interactions were seen for any of the cells tested. Although contrast sensitivity decreases monotonically with increasing temporal frequency, as would be predicted from data illustrated in Figs. 5B, 8, and 9, the shape of the spatial contrast sensitivity function and the position of the peak sensitivity are both always preserved across the range of temporal frequencies. Consequently, the X-cells continued to show a low spatial frequency attenuation in contrast sensitivity for all temporal frequencies, and Y-cells never did.

From these spatiotemporal contrast sensitivity functions, we calculated the change in spatial resolution as a function of temporal frequency. For a more convenient comparison among cells, the data were normalized in the following manner. The spatial resolution for different temporal frequencies was expressed as a proportion of the spatial resolution measured at 2 cycles/s; likewise, the temporal resolution for different spatial frequencies was expressed as a proportion of the temporal resolution measured at the most sensitive spatial fre-

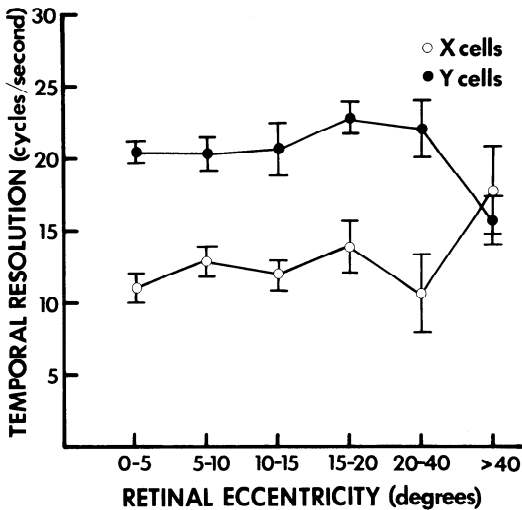


FIG. 10. Mean temporal resolutions of X- and Y-cells plotted as a function of receptive-field eccentricity from area centralis. The temporal resolution values were obtained using a sine-wave grating of 0.6 contrast, at a spatial frequency for which the cell exhibited the lowest contrast threshold (see text for details). Bars denote ± 1 standard error of the mean. Open circles indicate means for X-cells; filled circles, for Y-cells. The cell numbers represented by each point can be inferred from Fig. 11.

quency. These normalized spatiotemporal relationships are illustrated in Fig. 14 for the six X-cells and five Y-cells appropriately studied. Figure 14 indicates for both X- and Y-cells a linear reciprocal relationship between these variables; as temporal frequency increases, spatial resolution drops, and vice versa. For each X- and Y-cell measured, the correlation coefficient exceeded 0.9 ($P < 0.01$). The mean regression lines for the X- and Y-cell populations are shown in Fig. 14. The slopes are both roughly 45° and not significantly different ($P > 0.1$ on an F test), but the intercepts are significantly different ($P < 0.01$ on an F test).² Therefore, while we found no clear inverse relationship between spatial and temporal resolution within the X- or Y-cell

² The functions in Fig. 14 have been normalized as described above and, for this reason, the X- and Y-cell functions appear roughly parallel. If however, absolute values were used, the functions would cross. This would occur because, at low spatial frequencies, Y-cells on average exhibit much better temporal resolution than do X-cells, but at higher spatial frequencies (especially just above the resolution of Y-cells), X-cells on average display better (albeit poor) temporal resolution than do Y-cells.

populations, an inverse relationship appears to exist for individual cells between resolution (spatial or temporal) and the frequency (temporal or spatial, respectively) used to determine this resolution.

Relationship between center size and resolution

It has been suggested that the spatial-frequency response of visual neurons is related to the size of their receptive-field centers (10, 17, 18, 22). We investigated this possible relation by comparing the spa-

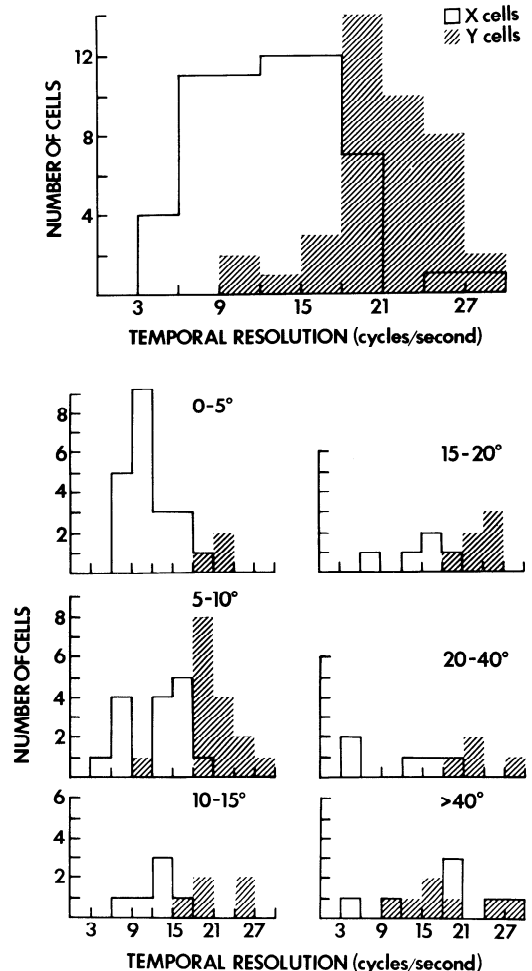


FIG. 11. Cell frequency distributions of temporal resolution for X- and Y-cells. The frequency distributions of temporal resolution for X- and Y-cells for all retinal eccentricities are shown in the upper part of figure. The frequency distributions of X- and Y-cells for six different retinal eccentricity groups are separately shown in the lower part of figure. Open frequency histograms indicate distributions for X-cells; cross-hatched, for Y-cells.

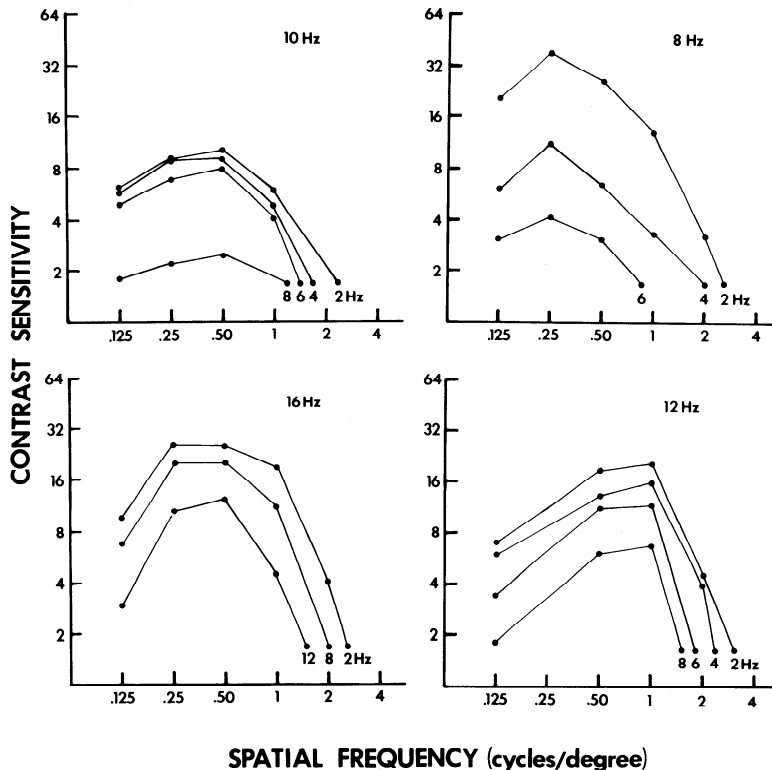


FIG. 12. Spatial contrast sensitivity functions plotted at a number of different temporal frequencies for four X-cells. The number in the upper right-hand corner of each plot denotes the temporal resolution of the cell. The number at the end of each contrast sensitivity function denotes the temporal frequency at which the spatial contrast thresholds were measured.

tial resolution of X- and Y-cells with the size of their receptive-field centers.

X-CELLS. We found a correlation between receptive field center diameter and the inverse of spatial resolution (deg/cycle) for X-cells. Figure 15A illustrates the relationship between hand-plotted center diameters and spatial resolution for our sample of X-cells. Although the correlation is significant ($r = 0.55$; $P < 0.01$), this relationship has little predictive value.

A possible source of error in this analysis is the relative imprecision of the hand-plotting methods. Indeed, receptive-field centers of X-cells are often tiny, and small differences in center diameter may not have been resolved. To investigate this possibility for nine X-cells, we also estimated center diameter from area-response functions. These measured neuronal response as a function of the area of a flashing spot of uniform intensity (33 cd/m² for stimulus-on versus 1 cd/m² for stimulus-off). The spots

were generated on the CRT, precisely centered on the field, and counterphased at 2 cycles/s. Computer-generated peristimulus histograms were used to measure neural responsivity. Figure 16A shows a typical area-response function for an X-cell, and the spot diameter that evokes the maximum discharge provides a reliable measure of receptive-field center diameter (cf. Ref. 21 and the legend to Fig. 16). Figure 16B shows normalized functions (see figure legend) for all of the nine X-cells studied, and Fig. 16C illustrates the relationships between hand plotting and area-response measures of center diameter. A significant correlation exists ($r = +0.75$; $P < 0.01$), but the area-response estimates of center size were consistently larger than were the hand-plotted ones.

Figure 15B plots the inverse of spatial resolution as a function of center diameter as measured from area-response functions. As in Fig. 15A, the correlation is significant

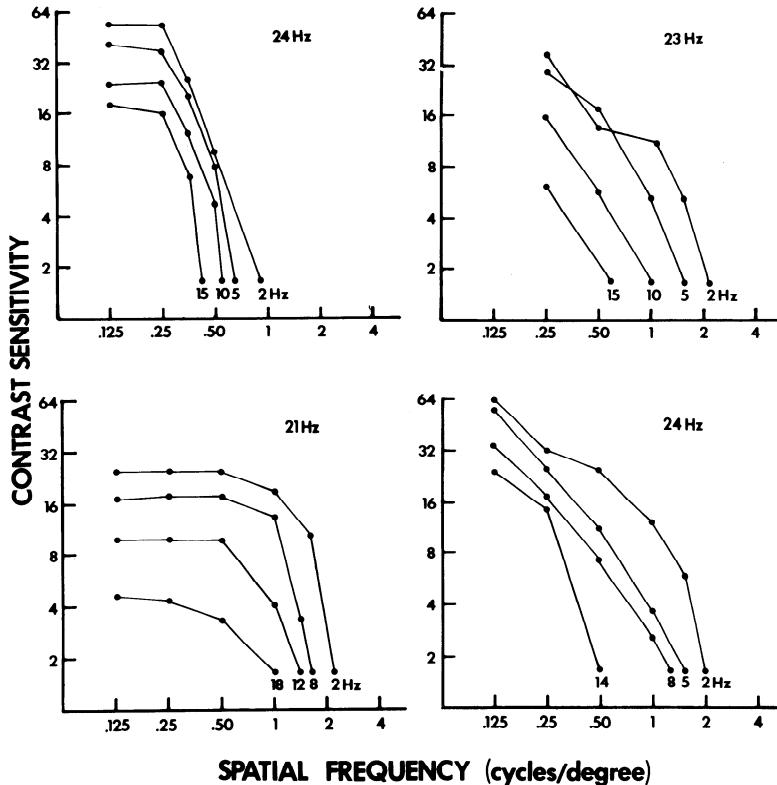


FIG. 13. Spatial contrast sensitivity functions plotted at a number of different temporal frequencies for four Y-cells; conventions as in Fig. 12.

($r = 0.62$; $P < 0.01$), but there is still little predictive value in this relationship. In fact, the correlations in Fig. 15A, B do not significantly differ from one another ($P > 0.1$ on a test of Z values). We conclude that the variability seen in Fig. 15A is not mainly due to inaccuracies limited to the hand-plotting procedures.

In addition to the fact that the correlation between spatial resolution and center size of X-cells is weak, there is another reason to suspect that the actual size of the center does not determine the spatial resolving power of X-cells. The size of the center of an X-cell is always much larger than the size of a single "bar" of a grating (half-cycle completely above or below the average luminance of the grating) whose spatial frequency is the spatial resolution of the cell. The average diameter of the center of the nine X-cells from which we obtained area-response functions is 1° of visual angle. The average width of a half-cycle of the grating noted as the spatial resolution of the cells is only 0.28° of visual angle. Since an

average X-cell can resolve the bars of a grating whose widths are less than one-third of its center diameter, this suggests that the spatial summation characteristics of the center, rather than center size, might be the underlying receptive-field property governing the spatial resolution of the cell.³ The size and spatial summation characteristics of the center are probably related because cells that have smaller receptive-field centers also tend to have centers with greater sensitivity to small stimuli, and this could explain the relationship between the spatial resolution and center size.

³ Since center diameter is larger than a half-cycle of the finest resolvable grating, we considered the possibility that a close relationship exists between center size and the spatial frequency to which the cell is most sensitive. For instance, the average center size (roughly 1°) readily predicts the average spatial frequency of the grating, which elicits the most sensitive response (roughly 0.5 cycle/deg). However, the correlation between the inverse of the most sensitive spatial frequency and hand-plotted center diameter is rather weak ($r = 0.50$; $P < 0.01$).

The area-response functions for X-cells display a characteristic sharp response decrement as the spot size enlarges beyond the optimal. This indicates a strong inhibition by the surround on the center response, and is consistent with the attenuation of X-cell contrast sensitivity at lower spatial frequencies.

No correlation was seen for X-cells between receptive-field center diameter (hand-plotted measures) and temporal resolution ($P > 0.1$).

Y-CELLS. The relationship between spatial resolution and receptive-field center diameter was analyzed for Y-cells as well, but the results are more complicated than they are for X-cells. Figure 17A plots spatial resolution as a function of hand-plotted center size; spatial resolution in this case, as previously, is the highest spatial frequency to which the cell responded at 0.6 contrast. The correlation is weak, but marginally

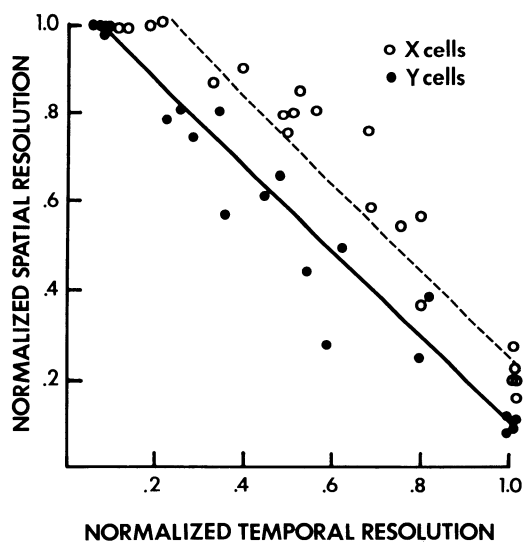


FIG. 14. Normalized spatiotemporal relations plotted for six X- and five Y-cells. The spatial resolution (at 2 cycles/s counterphase rate) and temporal resolution of each cell was first determined (see text), and these values for each cell were normalized to 1.0. Lower spatial and temporal frequencies are thus normalized at proportional values less than 1.0. Spatial (or temporal) resolution was then determined for each cell at different temporal (or spatial) frequencies, and these normalized values are plotted. Open circles denote these values for X-cells; filled circles, for Y-cells. The solid line represents the linear regression for these normalized values of spatial and temporal resolution for Y-cells. The broken line is the linear regression line for these normalized values for X-cells.

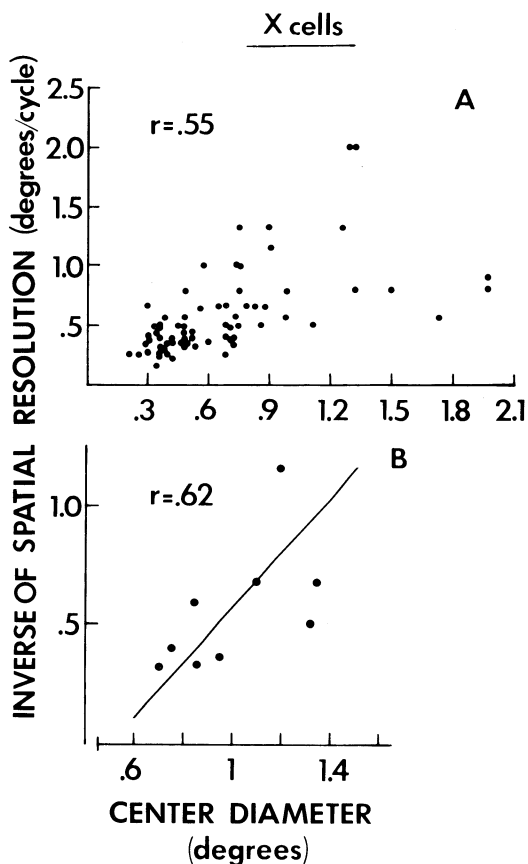


FIG. 15. Scatterplots of diameter of receptive-field center and inverse of spatial resolution for X-cells. The correlations between the inverse of spatial resolution and center diameter estimated by both techniques (hand-plotting and area-response functions) are shown in each scatterplot. *A*: inverse of spatial resolution as a function of center diameter measured by hand-plotting techniques. *B*: inverse of spatial resolution as a function of center diameter estimated from area-response functions. The linear regression line for these points is shown.

significant ($r = 0.4$; $P < 0.05$). As was done for certain X-cells, center size was estimated for six Y-cells by area-response functions (Fig. 18A, B), and these estimates did not correlate with hand-plotted estimates (Fig. 18C; $r = 0.15$; $P > 0.10$).⁴

⁴ It seems likely that the difficulty in estimating Y-cell center size contributes to this poor correlation. The relatively small response attenuation for larger spots indicates a weak surround inhibition of the center and makes the determination of the spot size for an optimal response difficult. Likewise, it is difficult for this reason to establish the center/surround boundary for Y-cells with hand-plotting methods.

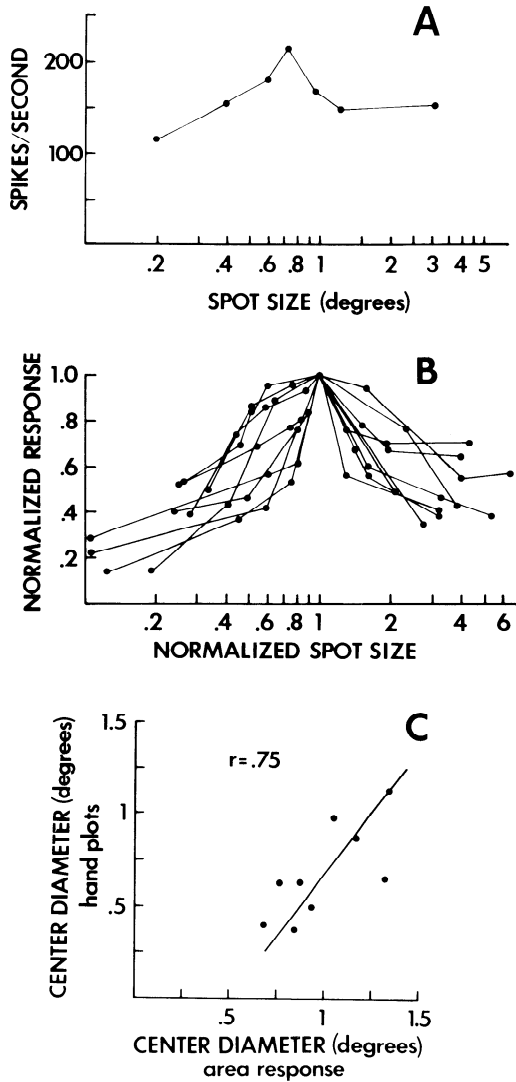


FIG. 16. Area-response functions for X-cells. *A*: typical function for an X-cell. This function is a plot of response magnitude measured in spikes per second for different spot sizes centered in the receptive field. The spot size that evokes the maximum response from the cell is taken as an estimate of size of the receptive-field center. For this cell, the center was estimated to be 0.7° of visual angle. *B*: normalized area-response functions plotted for nine X-cells. Response magnitude and spot size have been, respectively, expressed as a proportion of the magnitude of the maximum response and as a proportion of the spot size that elicited the maximum response. *C*: scatterplot of center diameters for nine X-cells estimated by hand plotting and by the area-response measures. The linear regression line for these points is shown, and the correlation coefficient is indicated. Area-response estimates of center diameter tend to be slightly larger than those based on hand plots.

Hochstein and Shapley (17, 18) have shown that Y-cell responses include two components. One component shows linear spatial summation, is thus dependent on spatial phase, and occurs at the fundamental temporal frequency of the stimulus (similar to X-cell responses); the other component does not show linear spatial summation, is independent of spatial phase, and occurs at even harmonics of the stimulus temporal frequency. The nonlinear component is more sensitive to higher spatial frequencies than is the linear component. Thus, by noting the transitional spatial frequency at which the responses shift from spatial phase dependence to independence, one can obtain a measure of the spatial resolution of the linear response component. For the above-mentioned six Y-cells from which area-

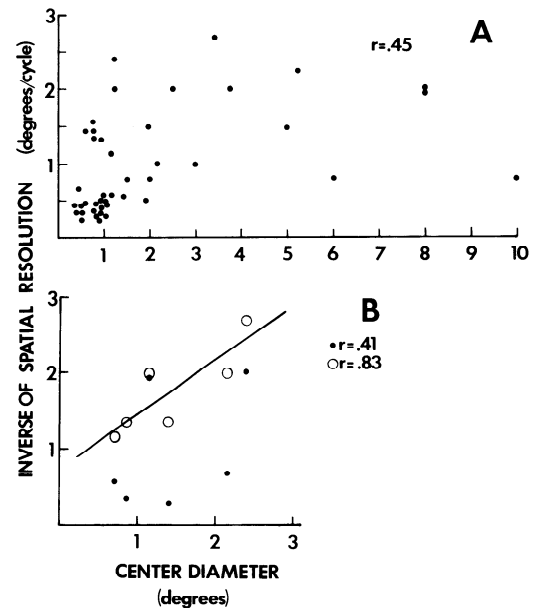


FIG. 17. Scatterplots of the receptive-field center diameter and inverse of spatial resolution for Y-cells. *A*: inverse of spatial resolution plotted as a function of center diameter measured by hand-plotting techniques. *B*: inverse of spatial resolution of the second harmonic response plotted as a function of center diameter estimated from area-response functions (filled circles); spatial resolution of the fundamental response plotted as a function of center diameter estimated from area-response functions (open circles). See text for details. The correlation coefficients are indicated. Center diameter correlates better with inverse of spatial resolution of the fundamental response, and the regression line is shown for this relationship.

response functions were obtained, we also measured two other spatial parameters: the spatial frequency at 0.6 contrast for which the responses shift from phase dependence to independence, and the spatial frequency (at 0.6 contrast), which represents the resolution of the nonlinear component. For most Y-cells, the transition from a phase-dependent to a phase-independent response was quite abrupt, but there always was a range of spatial frequencies for which an intermittent and weak phase dependence seemed present. The midpoint of this range was taken as an estimate of the linear component's resolution.

Figure 17B plots for these six Y-cells the area-response estimate of center diameter as a function of the inverse of spatial resolution, both of the nonlinear component (filled circles) as well as the linear component (open circles). The model of Y-cell receptive fields offered by Hochstein and Shapley (17, 18) suggests that the linear response component derives from a classical center/surround organization, whereas the nonlinear component derives from smaller spatial subunits distributed throughout the field. This is consistent with our observation that the inverse of spatial resolution of the linear component correlates rather well with center diameter ($r = 0.83$; $P < 0.01$), but that of the nonlinear component does not ($r = 0.41$; $P > 0.1$).

Note that the area-response functions for Y-cells (Fig. 18A, B) show very little decrement for spots larger than the optimal when compared to the decrement seen for X-cells. This suggests relatively little surround inhibition of the center response and is consistent with the lack of attenuation seen in the contrast sensitivity functions at low spatial frequencies (Fig. 4).

No correlation for Y-cells was seen between center diameter (hand-plotted measures) and temporal resolution ($P > 0.1$).

DISCUSSION

It has been suggested (e.g., Refs. 21, 22) that X-cells are most important for analyzing spatial patterns and Y-cells, for temporal patterns. The results of the present experiment, which indicate higher spatial resolu-

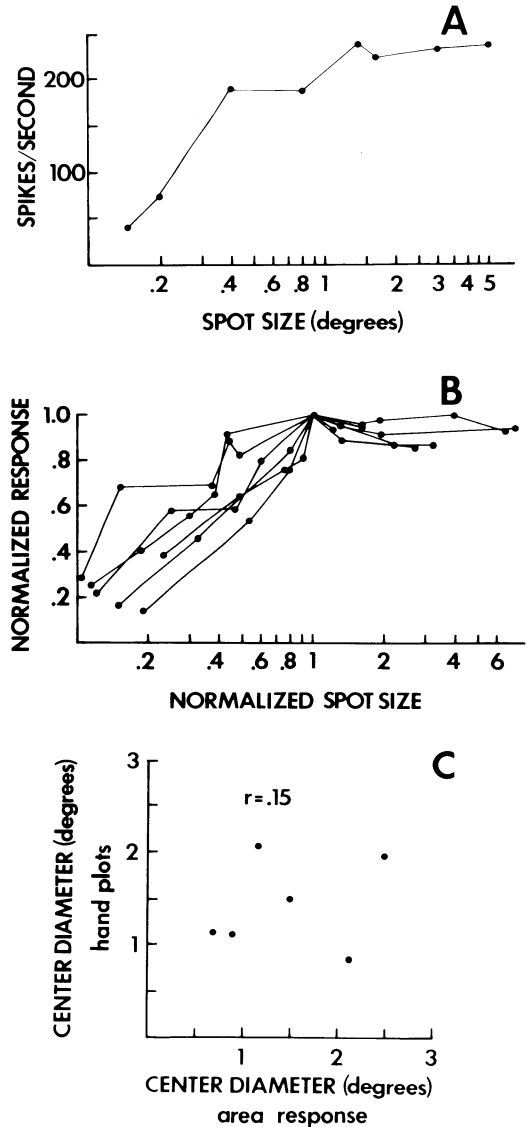


FIG. 18. Area-response functions for Y-cells. A: typical function for a Y-cell. B: normalized area-response functions plotted for six Y-cells (conventions as in Fig. 16B). C: Scatterplot of center diameters estimated by hand plotting and by area-response functions. The correlation between these estimates is not statistically significant.

tion on average for X-cells and higher temporal resolution on average for Y-cells, are not inconsistent with this notion. However, these differences are slight or unclear (see below) and less pronounced than other differences, which will be discussed and reiterated below.

Spatial properties

RESOLUTION. Bonds (5) has measured the optical modulation transfer function of the cat's eye with various-sized pupils and at retinal eccentricities up to 30° from the visual axis. From these data we can infer that the spatial resolution values and their decline with eccentricity observed in this study for X- and Y-cells are not limited by the cat's optics, but rather seem to have a neural origin. X-cells tended to exhibit slightly better spatial resolution than did Y-cells at all eccentricities, but considerable overlap was also evident. That is, some Y-cells responded to finer detail than did some X-cells at the same eccentricity, and more central fields of Y-cells showed better spatial resolution than more eccentric fields of X-cells. It thus seems unlikely to us that the key to the differential functional significance of X- and Y-cells depends on spatial resolution.

Most of our data are from cells with relatively peripheral fields for which spatial resolution tends to be lower. The highest resolution we obtained for an area centralis X-cell was 5.5 cycles/deg, and while this is consistent with some reports (2, 10, 19, 30), it is considerably lower than the 8 cycles/deg reported by Ikeda and Wright (23). It is possible that we failed to sample cells with higher spatial resolutions, but it should also be emphasized that subtle differences in the threshold determination for resolution between laboratories could contribute to differences in the absolute estimates of these values.

Our data for spatial resolution in Y-cells is best accommodated by the receptive-field model of Hochstein and Shapley (17, 18). They suggested a field comprised of a relatively linear center/surround organization, which dominates responses at the fundamental frequency, plus nonlinear subunits scattered throughout the field, which account for responses at the second harmonic. Since the second harmonic responses dominate at higher spatial frequencies, the Y-cell's spatial resolution presumably reflected the resolution of these nonlinear subunits. Furthermore, the spatial frequency above which the fundamental response attenuates and the second harmonic response dominates at all spatial phases presumably indicates

the spatial resolution of the more linear center/surround components. This is consistent with the clear correlation between this spatial frequency and center diameter for Y-cells.

Low spatial frequency sensitivity

Differences in responsiveness between X- and Y-cells are much more marked at low spatial frequencies than at higher ones (Figs. 3–5A). Y-cells are sensitive to low spatial frequencies, whereas X-cells are not. Therefore, Y-cells tend to respond well to a wide range of spatial frequencies until the spatial resolution is approached. X-cells, on the other hand, respond well only to a relatively narrow range of spatial frequencies.

Sensitivity to spatial phase

X-cells are extremely sensitive to spatial phase at all spatial frequencies. At phase angles near the null position, X-cells tend to exhibit poor sensitivity, and brisk responses would be elicited only for a relatively narrow range of grating locations. Y-cells, on the other hand, respond well regardless of the grating position. At higher spatial frequencies, the responses are essentially phase independent (see above and Refs. 17, 18). At lower spatial frequencies, the responses do depend on spatial phase, but still no null position is evident. That is, only the fundamental response will vary with grating position, but throughout these spatial variations, the cell would respond reasonably well due to second harmonic responses (17, 18).

Therefore, X-cells, on average, respond to slightly finer detail than can Y-cells. However, the X-cell responses are limited to a relatively small range of spatial frequencies and stimulus positions. Y-cells are relatively insensitive to such variations in spatial frequency or target position. From this, we might expect that a typical, complex visual scene, with a wide range of spatial frequencies and stimulus positions, would excite most Y-cells and proportionately few X-cells. Many X-cells would remain relatively unresponsive because the visual scene contains inappropriate spatial frequencies and/or stimulus locations.

Temporal properties

Analysis of temporal contrast sensitivity seems somewhat simpler than that of spatial

parameters. All of the lateral geniculate neurons of this study exhibited the same general temporal contrast-sensitivity functions. That is, sensitivity decreased at higher temporal rates and displayed no low-frequency reduction. Therefore, the main difference among cells was the temporal resolution. Temporal resolution of Y-cells was better than that of X-cells, on average, but variability and some overlap was evident.

It may be that this difference in average temporal resolution between X- and Y-cells is an artifact of our methods. As described in RESULTS, temporal resolution was measured at the spatial frequency to which the cell was most sensitive. As suggested by Fig. 3-5A, the spatial frequency chosen for X-cells (e.g., 1 cycle/deg) was typically greater than that for Y-cells (e.g., 0.25 cycle/deg). If instead of the most sensitive spatial frequency, we used a constant spatial frequency of, say 1 cycle/deg to measure temporal resolution in all cells, little difference between X- and Y-cells would be evident. X-cells would be relatively more sensitive to this spatial frequency than would Y-cells, and a replotting of the points in Figs. 10 and 11 would predict a reduced temporal resolution in Y-cells for a non-optimal spatial frequency. In other words, temporal sensitivity differences between X- and Y-cells are dependent on the spatial frequency used. At very low spatial frequencies (where X-cells display a sensitivity loss), Y-cell temporal resolution would be far better than that for X-cells; at moderate spatial frequencies, temporal resolution differences may disappear; and at higher spatial frequencies, X-cells would display better temporal resolution than would Y-cells (see footnote 2). In other words, these data do not support the general contention that Y-cells generally possess higher temporal resolution than do X-cells since absolute temporal resolution depends on the spatial frequency of the stimulus.

Functional considerations

The data from this and other studies have led us to suggest a hypothesis concerning the differential functional significance of X- and Y-cells. For reasons considered above, we find as not very compelling the suggestion that X-cells are needed to analyze spatial patterns and Y-cells, to analyze tem-

poral patterns. Rather, we suggest that Y-cells are essential to the analysis of spatial patterns and that X-cells add certain important details to this spatial information. Three general and independent lines of research have led us to this conclusion (see also Refs. 17, 18, 34).

First, recent work, which has measured the effects of spatial filtering on recognition of visual stimuli (13-16, 24), has shown that low spatial frequencies are responsible for the form information contained in a visual scene, whereas the high spatial frequencies are responsible for the fine detail in a scene. This work on spatial filtering has also shown that low spatial frequencies are sufficient for basic pattern recognition. For instance, if the high-frequency information is selectively filtered by blurring a visual stimulus, excellent pattern recognition remains. If the low frequencies are filtered as well (by diffusion, etc.), pattern recognition is severely impaired. Since Y-cells are more sensitive to these important low spatial frequencies, these cells could alone subserve basic spatial pattern vision. Since X-cells, on the other hand, are mainly more sensitive to high spatial frequencies, both because of their higher spatial resolution and low-frequency attenuation, these cells may be primarily responsible for processing the fine spatial detail.

Second, roughly selective removal of X- or Y-cells in cats suggests that Y-cells are essential to spatial pattern vision. Early lid suture seems to affect geniculate Y-cells much more than X-cells (29, 37), and these animals show a profound loss of spatial pattern vision (9, 11). This point is further developed in the following paper (28a). On the other hand, selective removal of X-cells causes mild deficits in the cat's spatial pattern vision. Geniculate X-cells project exclusively to area 17 (38), whereas Y-cells (including those in the medial interlaminar nucleus; Ref. 25) project as well to areas 18, 19, and lateral suprasylvian cortex (12, 29, 38). Lesions of area 17 (with perhaps minor involvement of area 18), which remove essentially all X-cell projections and leave many or most Y-cell projections intact, produce a cat with excellent spatial pattern vision and only a 20% loss of resolution (1). Furthermore, while Y-cells are re-

sponsive to fairly fine gratings, their phase-dependent (or position dependent) responses are limited to coarser gratings, while X-cells provide phase-dependent responses for all spatial frequencies. One would thus predict that a lesion of area 17 in a cat should affect minimally spatial resolution and appreciation of forms, but should have a much greater effect on perception of positional information. Consistent with this is the observation (1) that lesions of area 17, which only affect spatial resolution by 20%, create a much larger deficit in vernier acuity (i.e., the ability to detect whether or not two line segments are offset). Therefore, removing X-cells, which respond in a phase-dependent manner for all spatial frequencies, seems to affect spatial acuity less than vernier acuity. In addition, the better positional sensitivity of X-cells may have important implications for models dealing with the neural substrate of stereoscopic vision, since this perception of depth relies on the positional information provided by each eye.

Finally, as suggested above, proportionately more of the Y-cell population than the X-cell population would respond to typical, spatially complex visual scenes.

This is consistent with the notion that Y-cells perform a vital function in spatial pattern vision.

Our hypothesis, then, is that Y-cells provide the basic neural substrate for most spatial pattern vision. X-cells add certain details to this, such as higher spatial frequency analysis, better positional analysis, perhaps stereopsis, etc. Our evidence does not support the concept that X-cells essentially perform spatial analysis while Y-cells essentially perform temporal analysis.

ACKNOWLEDGMENTS

This work was supported by National Institutes of Health Grant EY 03038 and National Science Foundation Grant BNS77-06785.

K. E. Kratz and S. Lehmkuhle were supported by Public Health Service Individual Postdoctoral Fellowships DE 07037 and EY 05238, respectively. S. M. Sherman was supported by Public Health Service Research Career Development Award EY 00020.

Address reprint requests to: Dr. S. Murray Sherman, Dept. of Anatomical Sciences, SUNY, Stony Brook, School of Basic Health Sciences, Health Sciences Center, Stony Brook, New York 11794.

Received 28 March 1979; accepted in final form 2 July 1979.

REFERENCES

- BERKLEY, M. A. AND SPRAGUE, J. M. Striate cortex and visual acuity functions in the cat. *J. Comp. Neurol.* 187: 679-702, 1979.
- BISTI, S., CLEMENT, R., MAFFEI, L., AND MECACCI, L. Spatial frequency and orientation tuning curves of visual neurons in the cat: effects of mean luminance. *Exp. Brain Res.* 27: 335-345, 1977.
- BLAKE, R. AND CAMISA, J. Temporal aspects of spatial vision in the cat. *Exp. Brain Res.* 28: 325-333, 1977.
- BLAKE, R., COOL, S. J., AND CRAWFORD, M. L. S. Visual resolution in the cat. *Vision Res.* 14: 1211-1217, 1974.
- BONDS, A. B. Optical quality of the living cat eye. *J. Physiol. London* 243: 777-795, 1974.
- CAMPBELL, F. W., COOPER, G. F., AND ENROTH-CUGELL, C. The spatial selectivity of the visual cells of the cat. *J. Physiol. London* 203: 223-235, 1969.
- CLELAND, B. G., DUBIN, M. W., AND LEVICK, W. R. Sustained and transient neurones in the cat's retina and lateral geniculate nucleus. *J. Physiol. London* 217: 473-496, 1971.
- CLELAND, B. G., MORSTYN, R., WAGNER, H. G., AND LEVICK, W. R. Long latency retinal input to lateral geniculate neurones of the cat. *Brain Res.* 91: 306-310, 1975.
- DEWS, P. B. AND WIESEL, T. N. Consequences of monocular deprivation on visual behavior in kittens. *J. Physiol. London* 206: 437-455, 1970.
- ENROTH-CUGELL, C. AND ROBSON, J. G. The contrast sensitivity of retinal ganglion cells in the cat. *J. Physiol. London* 187: 517-552, 1966.
- GANZ, L. AND FITCH, M. The effect of visual deprivation on perceptual behavior. *Exp. Neurol.* 22: 683-690, 1968.
- GILBERT, C. D. AND KELLY, J. P. The projections of cells in different layers of the cat's visual cortex. *J. Comp. Neurol.* 163: 81-106, 1975.
- GINSBURG, A. *Visual Information Processing Based Upon Spatial Filters Constrained by Biological Data* (Dissertation). Cambridge: Univ. of Cambridge, 1977.
- GINSBURG, A. P., CARL, J. W., KABRISKY, M., HALL, C. F., AND GILL, P. A. Psychological aspects of a model for the classification of visual images. In: *Advances in Cybernetics and Systems*, edited by J. Rose. London: Gordon and Breach, 1976, p. 1289-1306.
- HESS, R. F. AND GARNER, L. R. The effects of corneal edema on visual function. *Invest. Ophthalmol. Vision Sci.* 16: 5-13, 1977.
- HESS, R. AND WOO, G. Vision through cataracts. *Invest. Ophthalmol. Vision Sci.* 17: 428-435, 1978.
- HOCHSTEIN, S. AND SHAPLEY, R. M. Quantitative

- aspects of retinal ganglion cell classifications. *J. Physiol. London* 262: 237–264, 1976.
18. HOCHSTEIN, S. AND SHAPLEY, R. M. Linear and nonlinear spatial subunits in Y-cat retinal ganglion cells. *J. Physiol. London* 262: 265–284, 1976.
 19. HOFFMANN, K.-P. AND SIRETEANU, R. Interlaminar differences in the effects of early and late monocular deprivation on the visual acuity of cells in the lateral geniculate nucleus of the cat. *Neurosci. Lett.* 5: 171–175, 1977.
 20. HOFFMANN, K.-P., STONE, J., AND SHERMAN, S. M. Relay of receptive-field properties in dorsal lateral geniculate nucleus of the cat. *J. Neurophysiol.* 35: 518–531, 1972.
 21. IKEDA, H. AND WRIGHT, M. J. Receptive field organisation of sustained and transient retinal ganglion cells which subserve different functional roles. *J. Physiol. London* 227: 769–800, 1972.
 22. IKEDA, H. AND WRIGHT, M. J. Spatial and temporal properties of sustained and transient neurones in area 17 of the cat's visual cortex. *Exp. Brain Res.* 22: 363–383, 1975.
 23. IKEDA, H. AND WRIGHT, M. J. Properties of LGN cells in kittens reared with convergent squint: a neurophysiological demonstration of amblyopia. *Exp. Brain Res.* 25: 63–77, 1976.
 24. KARRISKY, M., TALLMAN, O., DAY, C. M., AND RADOY, C. M. A theory of pattern perception based on human physiology. *Ergonomics* 13: 129–142, 1970.
 25. KRATZ, K. E., WEBB, S. V., AND SHERMAN, S. M. Studies of the cat's medial interlaminar nucleus: a subdivision of the dorsal lateral geniculate nucleus. *J. Comp. Neurol.* 180: 601–614, 1978.
 26. KRATZ, K. E., WEBB, S. V., AND SHERMAN, S. M. Electrophysiological classification of X- and Y-cells in the cat's lateral geniculate nucleus. *Vision Res.* 18: 489–492, 1978.
 27. KULIKOWSKI, J. J. AND TOLHURST, D. J. Psychophysical evidence for sustained and transient detectors in human vision. *J. Physiol. London* 232: 149–162, 1973.
 28. LEHMKUHLE, S. W., KRATZ, K. E., MANGEL, S., AND SHERMAN, S. M. An effect of early monocular lid suture upon the development of X-cells in the cat's lateral geniculate nucleus. *Brain Res.* 157: 346–350, 1978.
 - 28a. LEHMKUHLE, S. W., KRATZ, K. E., MANGEL, S. C., AND SHERMAN, S. M. Effects of early monocular lid suture on spatial and temporal sensitivity of neurons in dorsal lateral geniculate nucleus of the cat. *J. Neurophysiol.* 43: 542–556, 1980.
 29. LEVAY, S. AND FERSTER, D. Relay cell classes in the lateral geniculate nucleus of the cat and effects of visual deprivation. *J. Comp. Neurol.* 172: 563–584, 1977.
 30. MAFFEI, L. AND FIORENTINI, A. The visual cortex as a spatial frequency analyzer. *Vision Res.* 13: 1255–1267, 1973.
 31. MOVSHON, J. A., THOMPSON, I. D., AND TOLHURST, D. J. Spatial summation in the receptive fields of simple cells in the cat's striate cortex. *J. Physiol. London* 283: 53–77, 1978.
 32. MOVSHON, J. A., THOMPSON, I. D., AND TOLHURST, D. J. Receptive field organization of complex cells in the cat's striate cortex. *J. Physiol. London* 283: 79–99, 1978.
 33. MOVSHON, J. A., THOMPSON, I. D., AND TOLHURST, D. J. Spatial and temporal contrast sensitivity of neurones in areas 17 and 18 of cat's visual cortex. *J. Physiol. London* 283: 101–120, 1978.
 34. RODIECK, R. W. Visual pathways. *Annu. Rev. Neurosci.* 2: 193–225, 1979.
 35. ROWE, M. H. AND STONE, J. Naming of neurones: classification and naming of cat retinal ganglion cells. *Brain Behav. Evol.* 14: 185–216, 1977.
 36. SHAPLEY, R. AND HOCHSTEIN, S. Visual spatial summation in two classes of geniculate cells. *Nature London* 256: 411–413, 1975.
 37. SHERMAN, S. M. Visual development in cats. *Invest. Ophthalmol.* 11: 394–401, 1972.
 38. STONE, J. AND DREHER, B. Projections of X- and Y-cells of cats' lateral geniculate nucleus to areas 17 and 18 of visual cortex. *J. Neurophysiol.* 36: 551–567, 1973.
 39. WILSON, J. R. AND SHERMAN, S. M. Differential effects of early monocular deprivation on binocular and monocular segments of cat striate cortex. *J. Neurophysiol.* 40: 891–903, 1977.
 40. WILSON, P. D., ROWE, M. H., AND STONE, J. Properties of relay cells in cat's lateral geniculate nucleus: a comparison of W-cells with X- and Y-cells. *J. Neurophysiol.* 39: 1193–1209, 1976.